



Aalborg Universitet

AALBORG UNIVERSITY  
DENMARK

## Neutrophil extracellular traps in ulcerative colitis

*a proteome analysis of intestinal biopsies*

Bennike, Tue Bjerg; Carlsen, Thomas Gelsing; Ellingsen, Torkell; Bonderup, Ole Kristian; Glerup, Henning; Bøgsted, Martin; Christiansen, Gunna; Birkelund, Svend; Stensballe, Allan; Andersen, Vibeke

*Published in:*  
Inflammatory Bowel Diseases

*DOI (link to publication from Publisher):*  
[10.1097/MIB.0000000000000460](https://doi.org/10.1097/MIB.0000000000000460)

*Creative Commons License*  
CC BY-NC-ND 3.0

*Publication date:*  
2015

*Document Version*  
Publisher's PDF, also known as Version of record

[Link to publication from Aalborg University](#)

### *Citation for published version (APA):*

Bennike, T. B., Carlsen, T. G., Ellingsen, T., Bonderup, O. K., Glerup, H., Bøgsted, M., Christiansen, G., Birkelund, S., Stensballe, A., & Andersen, V. (2015). Neutrophil extracellular traps in ulcerative colitis: a proteome analysis of intestinal biopsies. *Inflammatory Bowel Diseases*, 21(9), 2052-2067.  
<https://doi.org/10.1097/MIB.0000000000000460>

### **General rights**

Copyright and moral rights for the publications made accessible in the public portal are retained by the authors and/or other copyright owners and it is a condition of accessing publications that users recognise and abide by the legal requirements associated with these rights.

- Users may download and print one copy of any publication from the public portal for the purpose of private study or research.
- You may not further distribute the material or use it for any profit-making activity or commercial gain
- You may freely distribute the URL identifying the publication in the public portal -

### **Take down policy**

If you believe that this document breaches copyright please contact us at [vbn@aub.aau.dk](mailto:vbn@aub.aau.dk) providing details, and we will remove access to the work immediately and investigate your claim.

# Neutrophil Extracellular Traps in Ulcerative Colitis: A Proteome Analysis of Intestinal Biopsies

Tue Bjerg Bennike, PhD,<sup>\*,†,‡</sup> Thomas Gelsing Carlsen, MS,<sup>\*</sup> Torkell Ellingsen, MD, PhD,<sup>§</sup>  
 Ole Kristian Bonderup, MD, PhD,<sup>||,¶</sup> Henning Glerup, MD, PhD,<sup>||</sup> Martin Bøgsted, PhD,<sup>\*\*,††</sup>  
 Gunna Christiansen, MD, DMSc,<sup>††</sup> Svend Birkelund, MD, PhD, DMSc,<sup>\*</sup> Allan Stensballe, PhD,<sup>\*</sup>  
 and Vibeke Andersen, MD, PhD<sup>†,‡,§§</sup>

**Background:** The etiology of the inflammatory bowel diseases, including ulcerative colitis (UC), remains incompletely explained. We hypothesized that an analysis of the UC colon proteome could reveal novel insights into the disease etiology.

**Methods:** Mucosal colon biopsies were taken by endoscopy from noninflamed tissue of 10 patients with UC and 10 controls. The biopsies were either snap-frozen for protein analysis or prepared for histology. The protein content of the biopsies was characterized by high-throughput gel-free quantitative proteomics, and biopsy histology was analyzed by light microscopy and confocal microscopy.

**Results:** We identified and quantified 5711 different proteins with proteomics. The abundance of the proteins calprotectin and lactotransferrin in the tissue correlated with the degree of tissue inflammation as determined by histology. However, fecal calprotectin did not correlate. Forty-six proteins were measured with a statistically significant differences in abundances between the UC colon tissue and controls. Eleven of the proteins with increased abundances in the UC biopsies were associated with neutrophils and neutrophil extracellular traps. The findings were validated by microscopy, where an increased abundance of neutrophils and the presence of neutrophil extracellular traps by extracellular DNA present in the UC colon tissue were confirmed.

**Conclusions:** Neutrophils, induced neutrophil extracellular traps, and several proteins that play a part in innate immunity are all increased in abundance in the morphologically normal colon mucosa from patients with UC. The increased abundance of these antimicrobial compounds points to the stimulation of the innate immune system in the etiology of UC.

(*Inflamm Bowel Dis* 2015;21:2052–2067)

**Key Words:** ulcerative colitis, neutrophil extracellular traps, inflammatory bowel diseases, proteomics, microscopy

Ulc erative colitis (UC), 1 of the 2 major forms of inflammatory bowel diseases (IBDs), is an important health problem. The incidence rate varies between the geographic regions, and in Europe, annual incidence rates between 0.6 and 24.3 per 10<sup>5</sup> inhabitants and prevalences rates between 4.9 and 505 per 10<sup>5</sup> inhabitants have been reported.<sup>1</sup> Ulcerative colitis has a great impact on the quality of life of the affected individuals and for

society due to lost labor and expenses to the health care system.<sup>2–4</sup> The etiology of IBD remains incompletely explained but involves genetic and environmental factors. Genome-wide association studies have reported 133 loci to be associated with UC, many of which are associated with defects in the immune system. Current knowledge supports that UC is caused by an inappropriate immune response to the commensal microorganisms

Received for publication February 26, 2015; Accepted March 27, 2015.

From the \*Department of Health Science and Technology, Aalborg University, Aalborg, Denmark; <sup>†</sup>Organ Center, Hospital of Southern Jutland, Aabenraa, Denmark; <sup>‡</sup>Institute of Regional Health Research-Center Sønderjylland, University of Southern Denmark, Odense, Denmark; <sup>§</sup>Department of Rheumatology, Odense University Hospital, Odense, Denmark; <sup>||</sup>Diagnostic Center, Section of Gastroenterology, Regional Hospital Silkeborg, Silkeborg, Denmark; <sup>¶</sup>University Research Clinic for Innovative Patient Pathways, Aarhus University, Aarhus, Denmark; <sup>\*\*</sup>Department of Clinical Medicine, Aalborg University, Aalborg, Denmark; <sup>††</sup>Department of Haematology, Aalborg University Hospital, Aalborg, Denmark; <sup>††</sup>Department of Biomedicine, Aarhus University, Aarhus, Denmark; and <sup>§§</sup>Department of Internal Medicine, Regional Hospital Viborg, Viborg, Denmark.

Supported by grants from Knud and Edith Eriksens Memorial Foundation and Ferring (V.A.); Obelske Family Foundation and the Svend Andersen Foundation (A.S.); Knud Hojgaard Foundation Denmark, the Lundbeck Foundation Denmark, the Oticon Foundation Denmark, and the Otto Monsteds Foundation Denmark (T.B.B.).

The authors have no conflicts of interest to disclose.

Reprints: Tue Bjerg Bennike, PhD, Department of Health Science and Technology, Aalborg University, Fredrik Bajers vej 3B, 9220 Aalborg, Denmark (e-mail: tbe@hst.aau.dk).

Copyright © 2015 Crohn's & Colitis Foundation of America, Inc. This is an open-access article distributed under the terms of the Creative Commons Attribution-NonCommercial-NoDerivatives 3.0 License, where it is permissible to download and share the work provided it is properly cited. The work cannot be changed in any way or used commercially.

DOI 10.1097/MIB.0000000000000460

Published online 19 May 2015.

living in the gastrointestinal tract, collectively termed the gut microbiota.<sup>5–10</sup>

Ulcerative colitis is characterized by superficial inflammatory changes limited to the mucosa and submucosa of the colon.<sup>5</sup> Markers of inflammation obtainable in feces or serum include C-reactive protein in serum and the proteins lactotransferrin and calprotectin in feces.<sup>11,12</sup> C-reactive protein may be increased during the active phase of UC and is mainly produced in the liver in response to stimulation by proinflammatory mediators produced at the site of inflammation. Lactotransferrin is involved in the mucosal innate immune system response. It is an iron-binding glycoprotein with antimicrobial properties and is expressed by activated neutrophils and is released by the injured tissue.<sup>13,14</sup> Calprotectin is a complex between the 2 proteins S100-A8 and S100-A9 and is involved in the recruitment of leukocytes. Additionally, calprotectin has antimicrobial activity toward bacteria and fungi and composes up to 60% of the soluble cytosol proteins in human neutrophils.<sup>15,16</sup> Increased abundance of fecal calprotectin is a sensitive marker for intestinal inflammation but has also been seen with the use of nonsteroidal anti-inflammatory drugs and increasing age.<sup>14</sup> The abundance of all 3 proteins increases in response to intestinal inflammation.

Accordingly, diagnostic and prognostic markers for IBD, which would be valuable tools that could significantly improve treatment outcome, are currently missing. In this project, we investigate protein changes in the intestinal tissue, in contrast to proteins released to the bloodstream or feces. The aim was to increase our knowledge of the UC etiology and to identify markers, which could be translated to clinical use. Several studies have investigated protein changes in the colon mucosa tissue. However, so far mainly gel-based techniques have been used where the proteins are separating based on mass and charge (isoelectric point). Subsequently, the proteins are stained and quantified, and up to hundreds of protein spots on the gel can be identified by mass spectrometry (MS).<sup>11</sup> One such study compared colonic biopsies from 4 patients with UC and 5 controls and identified 19 proteins with different abundance between the 2 groups, indicating that mitochondrial dysfunction might be involved in the UC etiology.<sup>17</sup> A more recent study compared inflamed and noninflamed colon biopsies from 20 patients with UC and identified 43 proteins that differentiated between the 2 conditions, many of which were involved in energy metabolism and oxidative stress.<sup>18</sup> The 2-dimensional gel-based techniques allow for visual identification of regulated proteins and protein products that differ between different samples by image analysis followed by MS protein identification. However, 2-dimensional gel-based techniques are laborious and are limited to the identification of protein spots in the hundreds. The identification of non-changing proteins is for that reason often omitted from the analysis.<sup>11,19</sup>

In a recent study of patients with UC by Han et al,<sup>20</sup> a gel-free liquid chromatography (LC)-MS technique is used to analyze protein changes in colonic biopsies, which led to the identification

of 339 proteins.<sup>20</sup> Several of the proteins were involved in inflammation and cytoskeleton rearrangement. However, based on the number of visualized protein spots from the gel-based studies, we can expect the colonic biopsies to contain different proteins in the thousands. The gel-free LC-MS study has, therefore, merely identified a fraction of the proteins, and high-throughput proteomics technologies can be used to further identify and quantify disease-specific proteins.<sup>11</sup> We performed a proteomics study of morphologically normal intestinal tissue from patients with UC, and we found it important to use a current state-of-the-art proteomics platform for high-throughput protein identification and quantitation in the colon mucosa.

## MATERIALS AND METHODS

### Study Cohort

The study cohort size was determined based on a power analysis. Initially, we assumed that approximately 6000 *t* tests were to be performed in the study with an effect chance of 0.01. Based on this, 10 subjects in each group to be compared yields an estimated power of 95% to detect an effect size of 2.5 when correlating with Benjamini and Hochberg.<sup>21</sup> Therefore, 10 patients with UC for whom endoscopy was planned and 10 healthy subjects were recruited at the outpatients clinic, Diagnostic center Regional Hospital Silkeborg in the period from 2012 to 2013. Diagnosis of UC was based on standard clinical, endoscopic, and histological criteria, and an infectious etiology was excluded.<sup>22</sup> Information on diagnosis, medication, most recent fecal calprotectin measurement, and smoking habits was recorded from the patient records.

Written informed consent was obtained from all participants before participation in the study, and the project was approved by The Regional Scientific Ethical Committee (S-20120204) and the Danish Data Protection Agency (2008-58-035).

### Samples Collection

Biopsies for the histological evaluation of disease severity were sampled from descending colon, sigmoid colon, and rectum. Three biopsies were taken from each location. The biopsies were immediately placed on mixed cellulose ester filters (Advantec, Japan), fixed in phosphate-buffered 4% formaldehyde, and stored at room temperature until tissue sample preparation 24 hours later. Colon mucosal biopsies for MS were sampled 40 cm from the anus by sigmoidoscopy. Patient biopsies were taken from macroscopically normal tissue, and all controls had normal findings at sigmoidoscopy. The biopsies were immediately transferred to cryotubes and snap-frozen in liquid nitrogen followed by storage at –140°C until proteomics sample preparation.

### Sample Preparation for Histology

The formalin-fixed biopsies were paraffin embedded, sliced in 10 µm, deparaffinized with tissue clear (Sakura, AJ Alphen aan den Rijn, The Netherlands), and stained with

hematoxylin and eosin (H&E) (Sigma-Aldrich, St. Louis, MO)<sup>23</sup> or incubated with 2 μM TO-PRO-3 (Thermo Scientific, Waltham, MA) in phosphate-buffered saline for 30 minutes, washed 3 times in phosphate-buffered saline, and mounted.

The H&E-stained slices were investigated with a DM5500B microscopy (Leica Camera, Solms, Germany) equipped with PL Floutar ×16/0.5, and ×40/1.00 objectives and Retiga 2000R CCD Camera (Qimaging, Canada), and the TO-PRO-3 microscopy was performed on a SP5 confocal microscope (Leica Camera) with a PL Floutar ×16/0.5, HCX PL APO ×63/1.40, and HCX PL APO ×100/1.47 objectives. The pictures were processed with ImageJ with the LOCI Tools plugin.<sup>24</sup>

### Colon Inflammation Grade Score

As part of the routine patient care at Regional Hospital Silkeborg, pathologists performed histological descriptions of formalin-fixed paraffin-embedded H&E-stained biopsies from descending colon, sigmoid colon, and rectum. The biopsies were characterized and assigned a colon inflammation grade score (0 = no disease activity, 1 = light activity, 2 = moderate activity, and 3 = severe activity) based on the histological descriptions (Table 1).<sup>18,25</sup> The sum of scores from the descending colon, sigmoid colon, and rectum were squared to yield patient colon inflammation grade scores. The scores were compared with the relative abundance of known inflammatory proteins in the tissue, and Pearson's correlation coefficients were calculated. The histological evaluation was supervised by a specialist in human pathology, blinded for the result of the proteomic analyses.

### Sample Preparation for Proteomics

The intestinal biopsies and lysates were kept on ice when possible. Each biopsy was homogenized with steel beads in 0.5 mL of cold lysis buffer (5% sodium deoxycholate, 50 mM

triethylammonium bicarbonate, pH 8.5), using intense shaking on a Precellys 24 homogenizer (Berting Technologies, Rockville, MD). The protein concentrations of the lysates were estimated by measuring absorbance at 280 nm (A280) using a NanoDrop 1000 UV-Vis spectrophotometer (Thermo Scientific). To increase the accuracy of the A280 estimations, the concentration of 4 biopsy lysates were determined using a bicinchoninic acid assay with bovine serum albumin as standard, measured using an Infinite microplate reader (Tecan, Männedorf, Switzerland). All A280 measurements were postprocessing calibrated using the bicinchoninic acid assay protein determinations.

Protein digestion was performed using a modified filter-aided sample preparation protocol.<sup>26–28</sup> A biopsy lysate volume corresponding to 100 μg of total solubilized protein was prepared for LC-MS analysis for each biopsy. Proteins were reduced for 30 minutes at room temperature by adding tris(2-carboxyethyl)phosphine (Thermo Scientific) to a final concentration of 10 mM. The reduced protein solution was transferred to a 30-kDa molecular weight cutoff spin-filter (Millipore, Billerica, MA), and buffer exchange was facilitated between all steps by centrifugation at 15,000g for 15 minutes at 4°C. The proteins were alkylated using 100 μL of 50 mM 2-iodoacetamide (Sigma-Aldrich) in lysis buffer. Two micrograms of sequencing grade modified trypsin (Promega, Madison, WI) dissolved in 50 μL of digestion buffer (0.5% sodium deoxycholate, 50 mM triethylammonium bicarbonate, pH 8.5) was added to the spin-filter, and the proteins were digested to peptides overnight at 37°C. The peptide material was eluted from the spin-filter and purified by phase inversions. One milliliter of ethyl acetate with 1% formic acid was added to the peptide material, the tube was vortexed, centrifuged at 15,000g for 5 minutes to obtain phase separation, and the aqueous phase with peptides was recovered.<sup>26,29</sup> The final peptide eluent was dried down in a vacuum centrifuge overnight and stored at –80°C until time of analysis.

**TABLE 1.** Disease Activity of Patients with UC

Patient	Histological Grading			Colon Inflammation Grade Score	F-Cal (μg/g)	F-Cal and Biopsy Time Difference (d)	Year of Diagnosis
	Descendens	Sigmoideum	Rectum				
UC_1	2	2	2	36	1285	7	2008
UC_2	0	0	1	1	889	20	2010
UC_3	1	2	2	25	1343	0	2003
UC_4	0	0	1	1	>3600	0	2010
UC_5	0	0	0	0	<30	28	2009
UC_6	0	2	0	4	705	0	2006
UC_7	2	1	3	36	575	117	2008
UC_8	0	2	0	4	163	37	2011
UC_9	2	0	0	4	<30	4	2000
UC_10	2	1	1.5	20.25	2060	5	2010

The histological grading of biopsies from colon descendens, colon sigmoideum, and rectum is used to calculate the colon inflammation grade score. Colon inflammation grade score = (descendens score + sigmoideum score + rectum score)<sup>2</sup>. Additionally, the measured fecal calprotectin (F-Cal) and the time difference between the measured F-Cal and the biopsy extraction are given.

## Proteomics—Analysis

Before LC-MS analysis, the dry peptide product was reconstituted in 20  $\mu$ L of 2% acetonitrile and 0.1% formic acid. Five micrograms of peptide material as determined by A280 was analyzed per LC-MS analysis. All biopsies were analyzed in triplicates and in a random order of biopsy analysis.<sup>30</sup>

The peptides were analyzed by LC-MS using an UltiMate 3000 UPLC system (Thermo Scientific) coupled online to a Q Exactive mass spectrometer (Thermo Scientific) using a trapping column setup. The peptide material was loaded onto a 2-cm trap column packed with Acclaim PepMap100 C18, 5  $\mu$ m 100  $\text{\AA}$  material (Thermo Scientific). Subsequently, the peptides were separated using a 50-cm analytical column packed with Acclaim PepMap100 C18, 2  $\mu$ m 100  $\text{\AA}$  material (Thermo Scientific). The peptides were eluted from the column with a gradient of 96% solvent A (0.1% formic acid) and 4% solvent B (0.1% formic acid in acetonitrile), which was increased to 8% solvent B on a 5-minute ramp gradient and subsequently to 30% solvent B on a 225-minute ramp gradient, with a constant flow rate of 300 nL/min. The column was washed with 90% solvent B for 10 minutes and equilibrated for 40 minutes, resulting in a total analysis time of 290 minutes per LC-MS analysis. Both columns were kept at 40°C. The eluting peptides were introduced directly into the mass spectrometer by a picotip emitter for nanoflow ionization (New Objective, Woburn, MA). The mass spectrometer was operated in positive mode using a data-dependent acquisition method. A full MS scan in the mass range of m/z 400 to 1200 was acquired at a resolution of 70,000. In each cycle, the mass spectrometer would trigger up to 12 MS/MS acquisitions of eluting ions based on highest signal intensity for fragmentation. The MS/MS scans were acquired with a dynamic mass range at a resolution of 17,500. The precursor ions were isolated using a quadrupole isolation window of 1.6 m/z and fragmented using high-energy collision with a normalized collision energy of 27. Fragmented ions were dynamically added to an exclusion list for 30 seconds.

## Proteomics—Raw File Analysis

The measured peptide signal intensities from the full MS scan were integrated using MaxQuant 1.4.1.2 software<sup>31,32</sup> and used to calculate the relative protein quantities (label-free quantitation). The fragment scans were searched against a UniProt database containing all reviewed *Homo sapiens* proteins (downloaded October, 8, 2013, containing 20,277 entries). The following abundant peptide modifications were included in the analysis: carbamidomethylated cysteine residues (fixed), acetylation of N peptides from the N-terminal of proteins (variable), oxidation of methionine (variable), and deamidation of asparagine and glutamine residues (variable).<sup>33,34</sup>

## Proteomics—Protein Data Processing

A target-decoy fragment spectra search strategy was applied and used to adjust the false discovery rate of identified

peptides and proteins to below 1% false discovery rate. For quantified proteins, additional filtering of the protein and peptide data was done to ensure high-quality quantitative data: (1) The quantitation of any protein was required to be based on at least 2 sequence-unique quantifiable peptides. (2) The sequence-unique peptides were required to be quantifiable in at least half of the UC biopsies or the control biopsies. (3) All biopsies had been analyzed in triplicates on the LC-MS system. To remove replicate analyses with poor repeatability, all measured protein abundances were log2 transformed and the repeated analyses were investigated individually for the biopsies by scatter plots. Ideally, the repeated analysis of a biopsy should yield identical protein abundances, represented by a Pearson's correlation coefficient of 1 in the scatter plots, indicating a perfect correlation. Individual replicate analyses with a Pearson's correlation less than 0.95 were removed from further analysis, to ensure that only highly reproducible replicates were included in the final data set. (4) To further identify replicate outliers, a principle component analysis (PCA) was performed in Perseus v1.4.1.3. The input for the PCA was all measured protein abundances in all replicates. For the purpose of conducting PCA, missing values (i.e., proteins where a quantitation value was not obtained for a given replicate analysis) were replaced with values from a normal distribution (width 0.3 and down shift 1.8) to simulate signals from low abundant proteins.<sup>35</sup> The grouping of the replicates on the calculated scores plots was investigated. Gene ontology annotations were imported from Uniprot Knowledgebase for all quantified proteins using STRAP v1.5 to classify the proteins.<sup>36</sup>

## Proteomics—Statistical Analysis

The repeated measurements of protein abundances were combined in Perseus v1.4.1.3 by taking the median biopsy wise, and the biopsies were grouped according to disease state: 10 biopsies from patients with UC and 10 from controls. To identify proteins with a statistically significant mean abundance change between the UC group and the control group, 2-sided *t* tests were performed. As several thousand *t* tests were performed, we applied permutation-based false-positive control to correct for multiple hypothesis testing (parameters:  $s_0 = 1$ , 250 randomizations).<sup>37–39</sup> Up to 15% of the statistically significantly changing proteins were allowed to be false positives (i.e., the measured average protein abundance is not statistically significantly different between the UC group and the control group) to ensure sufficient input for the downstream protein functional analysis.<sup>37</sup> Proteins displaying a statistically significant mean abundance change were further investigated using SPSS statistics v22 (IBM, Armonk, NY). The MS data have been deposited to the ProteomeXchange Consortium (<http://proteomecentral.proteomexchange.org>) by means of the PRIDE partner repository with the data set identifier PXD001608.<sup>40,41</sup>

**TABLE 2.** Study Cohort Information and Analysis

ID	Age	Gender	Smoking	Smoking History	Medicine (per day)
UC_1	27	Male		Never	Asacol (5-aminosalicylic acid) 1600 + 800 + 1600 mg
UC_2	45	Male		Stopped 2009	Asacol (5-aminosalicylic acid) 1600 mg × 2
					Asacol (5-aminosalicylic acid) suppository 500 mg
UC_3	44	Male		Stopped 2000	Imurel (azathioprine) 150 mg × 1
UC_4	45	Female		Stopped 2005	Pentasa (5-aminosalicylic acid) suppository 1 g
UC_5	26	Female	10 cigarettes per day	Current	Mesalal (5-aminosalicylic acid) suppository 500 mg
UC_6	70	Female		Stopped 1998	Mesalal (5-aminosalicylic acid) suppository 500 mg
UC_7	62	Male		Stopped 2009	Imurel (Azathioprin) 100 mg; Pentasa (5-aminosalicylic acid) 2000 mg
UC_8	36	Male		Never	Asacol (5-aminosalicylic acid) 1600 mg × 2
					Asacol (5-aminosalicylic acid) suppository 500 mg
UC_9	68	Female	10 cigarettes per day	Current	Asacol (5-aminosalicylic acid) 1600 mg × 2
UC_10	22	Female		Never	Asacol (5-aminosalicylic acid) 1600 mg × 2
					Asacol (5-aminosalicylic acid) suppository 500 mg
					Pred-Clysma (glucocorticoid) 24 mg
Ctrl_1	54	Male		Never	
Ctrl_2	27	Male		Never	NovoRapid (insulin)
Ctrl_3	42	Male		Never	
Ctrl_4	48	Male		Never	
Ctrl_5	54	Female		Stopped 1992	
Ctrl_6	27	Female		Stopped 2011	
Ctrl_7	42	Female		Never	
Ctrl_8	23	Male		Never	
Ctrl_9	28	Male		Never	
Ctrl_10	31	Male		Stopped 2008	

Age and gender were not found to be statistically significantly different ( $P > 0.05$ ) between the patients with UC (n = 10) and the controls (n = 10) as determined by 2-sided *t* tests.

## RESULTS

### Patient Material

The recorded medical information (Table 2) revealed 9 patients receiving 5-aminosalicylic acid, 2 patients receiving azathioprine, and 1 patient receiving glucocorticoid treatment, whereas 1 control received insulin treatment. The study cohort age, gender, and current smoking status was not found to be statistically different between the patients with UC and controls. However, the number of former smokers was increased in the UC group.

### Histological Analysis

To assess cell density and tissue morphology in the extracted biopsies, we investigated the H&E-stained sections by light microscopy (Fig. 1). The crypt architecture was preserved in all control samples and all UC biopsies. However, we observed an increased number of stained cell nuclei between the intestinal crypts in the biopsies from patients with UC compared with controls. The majority of cells between the intestinal crypts had segmented cell nucleus, a characteristic of polymorphonuclear neutrophils (PMNs).<sup>42,43</sup> As the biopsies for the proteome analysis

were obtained in parallel, we expect these biopsies to have the same characteristics.

### Proteomics Verification

Before homogenization of the biopsies for proteomics sample preparation, the average wet weight of the biopsies was measured to be 4.9 mg (3.6–5.9 mg; 25th–75th percentiles). Following homogenization of the biopsies in lysis buffer, the protein concentration of the lysate was measured and the average extracted protein yield, calculated from the biopsy wet weight, was 10% (9%–11%; 25th–75th percentiles), indicating an efficient and reproducible homogenization.

The proteins in each homogenized sample were digested to peptides using the filter-aided sample preparation protocol, and the complex peptide material was analyzed by LC-MS/MS with label-free quantitation.<sup>31,32</sup> During the 290-minute analysis of each homogenized and digested sample, the MS system detected peptide elution from the LC column and selected up to 12 precursor ions per MS cycle for fragmentation (Fig. 2). By bioinformatics analysis, the proteins were subsequently identified and quantified. To investigate the repeatability of the LC-MS analysis,

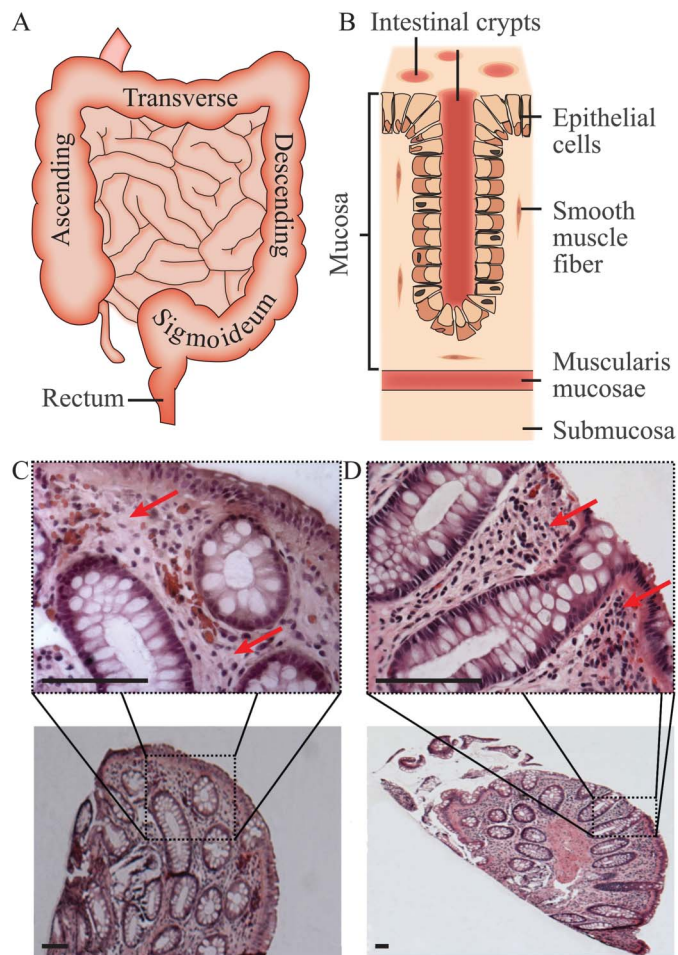


**FIGURE 1.** Biopsy histology analysis. **A**, Overview of the human small and large intestine. **B**, Cross section of a human colon. Representative H&E-stained colon biopsy slices from **(C)** control Ctrl\_10 and **(D)** patient UC\_05. The crypt architecture is in both slices preserved. However, an increased number of stained cell nuclei surrounding the crypts (red arrows) are apparent in the UC biopsies compared with the control biopsies (scale bars 100  $\mu$ m).

the technical triplicate analyses of each biopsy were analyzed by scatter plots, plotting the abundance of each quantified protein in one replicate against the same protein abundance as determined in other replicates, biopsy wise. Ideally, the repeated analysis should yield identical protein abundances, represented by a Pearson's correlation coefficient of 1 (Fig. 3A). Of the 60 LC-MS analyses, only 1 replicate from UC\_4 and 1 from UC\_5 had coefficients less than 0.95 and the 2 outlying replicates were removed from further analysis. The result demonstrates a high degree of technical repeatability of the method, that is, a low variance of the measured protein abundances when the same biopsy is analyzed repeatedly. To investigate how the measured protein abundances varied between all replicates and identify which replicates yielded similar protein abundances, a PCA was performed. A PCA is a statistical analysis technique that allows for reducing a large number

of variables to a smaller number of groups (principle components), which can be visualized on scores plots and used to interpret the variance in a complex data set, like that of high-throughput proteomics.<sup>44</sup> All measured protein abundances in all LC-MS analyses were used as input for the PCA, and 2-dimensional scores plots were constructed (Fig. 3B). The scores plot describes how the replicates group relative to one another, based on the differences in measured abundances of all proteins. In effect, replicates where similar protein abundances have been measured will be close in space on the scores plot, relative to the other replicates, and the PCA scores plot can thus be used to identify outliers. The PCA, thereby, includes the variance between all biopsies, unlike the scatter plots that only take the variance in the repeated analysis of the individual biopsies into account. Principal component 1 and principle component 2 represent the largest and second largest variance in the protein abundance data set, respectively, and explain 35.4% of the variance in the protein abundance data set. In all cases, the scores plot separates all biopsies from one another, in contrast to the repeated triplicate analysis of each biopsies, which group together for each individual biopsy (Fig. 3B, circles). This indicates that the measured protein abundances are more similar when the same biopsy is analyzed repeatedly than when different biopsies are analyzed. The variance in protein abundances between the different biopsies, therefore, is larger than the technical variance when the same biopsy is analyzed repeatedly, as expected for sensitive methods that validate the methodology.

### Proteomics—Data Analysis

Applying our strict criteria, 5711 quantifiable proteins remained postfiltering. The quantifiable proteins were classified by biological function, subcellular location, and molecular function, using available data from Uniprot Knowledgebase and gene ontology database (Fig. 4). The analysis of the biological processes performed by the proteins revealed that 68% of the quantified proteins were involved in cellular processes, such as intracellular communication; 55% of the proteins were involved in modulation of the frequency, rate, or extent of any biological process, quality, or function; and 29% were involved in metabolic processes, which include anabolism and catabolism by which living organisms transform chemical substances. We next investigated the cellular component of the proteins, that is, which parts of a cell or its extracellular environment the protein has been reported to be present. A somewhat even distribution was found between proteins associated with the cell cytoplasm, the cell nucleus, and the extracellular environment of the cell with 48%, 42%, and 35%, respectively. Finally, we investigated which primary molecular functions the proteins took part of. The analysis revealed that 68% of the proteins were involved in selective, non-covalent binding with other molecules, and 41% were involved in biologically catalyzed reactions. Based on the protein classification analysis, the quantified proteins originate from all cellular compartments, indicating that no systematic loss of proteins has occurred using the protocol and thus an unbiased analysis.

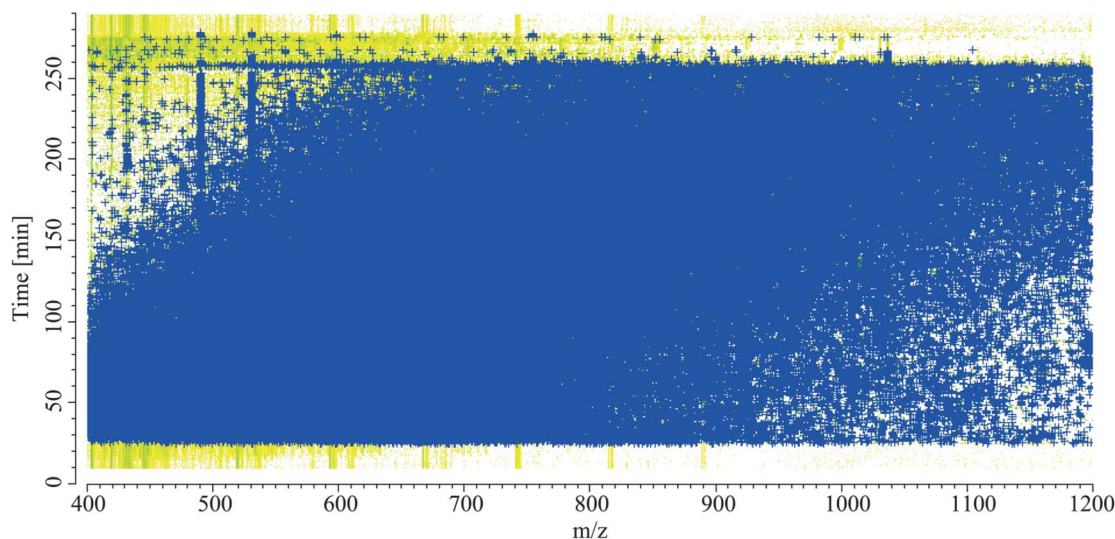


**FIGURE 2.** Representative 2-dimensional plot of the liquid chromatography-mass spectrometry analysis of patient UC\_9 illustrating the complexity of the analyzed peptide material. On the x-axis, the intensities of the peptide ion signals of the 19,549 acquired full MS scans are plotted, with a color gradient from white to green. The time of analysis is given on the y-axis. Each full MS scan was succeeded by up to 12 MS/MS scans of ions detected on the full MS scan and each cycle time was approximately 1 second; + indicates that the given ion signal was selected for MS/MS analysis, which came to 119,560 MS/MS scans in this 1 replicate.

Next, we analyzed the quantitative information obtained about the proteins in each biopsy. The measured protein abundances in the biopsies from the patient with UC were compared with the abundances in the biopsies from the control group, and *t* tests were performed to identify proteins with a statistically significant mean abundance change between the 2 groups. Forty-six proteins demonstrated a statistical significant mean abundance change between the UC biopsies and the control biopsies. All the 46 proteins were measured with an abundance

that, on average, was different between the UC biopsies and control biopsies by a factor of 2.8 or more, which is referred to as the fold change. Of the 46 proteins, 33 proteins were more abundant in the UC biopsies and 13 proteins were less abundant (Table 3). The protein with the largest mean fold abundance change between the UC and control biopsies was lactotransferrin, which was 219 times more abundant in the UC group. To further validate the measured protein abundances, we correlated the relative abundance of lactotransferrin and calprotectin with the severity of

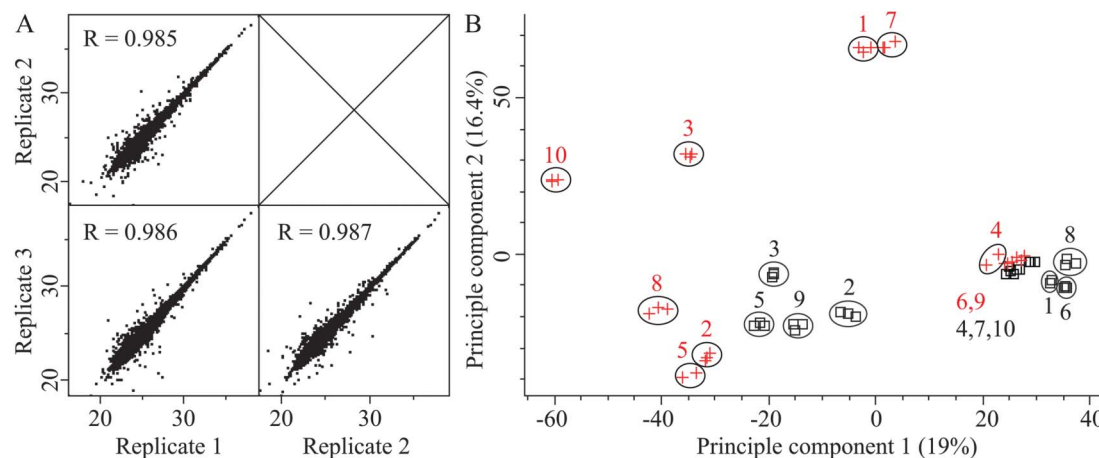


**FIGURE 3.** Proteomics data verification. A, Representative scatter plot of the triplicate biopsy analysis of UC\_1 of the 5711 quantified proteins. The log<sub>2</sub> transformed protein abundances of all proteins in replicates 1, 2, and 3 are plotted against one another on the x- and y-axes, respectively. Ideally, the measurements should yield identical protein abundances, represented by a Pearson's correlation coefficients (R) of 1. B, PCA scores plot of principle components 1 and 2 of the protein abundances as measured in the UC replicates (+) and control replicates (□). Technical replicates (encircled) group together in all cases, demonstrating a high degree of technical repeatability of the method. The study cohort subject ID is given as numbers (e.g., red 3 at [+] equals UC\_3) (Table 2).

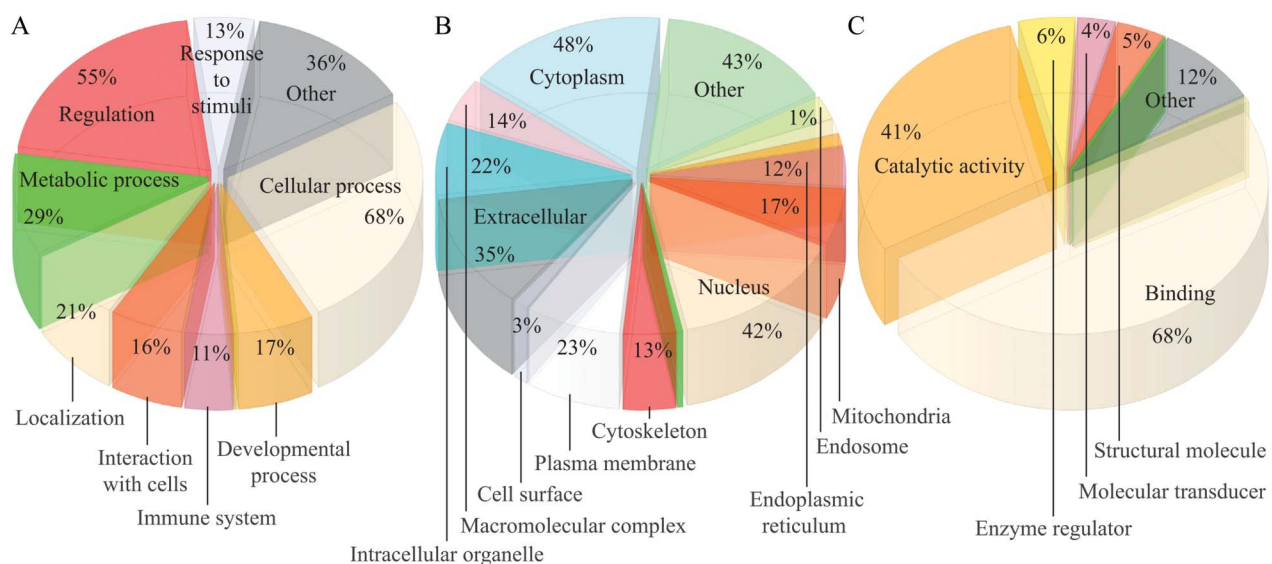


**FIGURE 4.** Gene ontology characterization of the 5711 quantified proteins in terms of (A) biological processes performed by the proteins, (B) cellular component to which the proteins are associated, and (C) the primary molecular functions of the proteins.

tissue inflammation in the patients with UC, as determined by histology. Both proteins are used to monitor UC disease activity.<sup>11</sup> Biopsies from descending colon, sigmoid colon, and rectum were assigned a colon inflammation grade score based on histology descriptions (Table 1). A good correlation was found between the colon inflammation grade scores and the relative abundance of calprotectin and lactotransferrin in the tissue, with Pearson's correlation coefficients of 0.84 and 0.91 for S100-A8 and S100-A9 protein, respectively, and 0.82 for lactotransferrin (Fig. 5). Finally, we correlated the relative abundance of calprotectin in the tissue to the most recent measure of fecal calprotectin as determined by routine tests. However, no correlation could be found, and a Pearson's correlation coefficient of 0.33 was calculated (data not shown).

Eleven of the 46 proteins with statistically significantly altered abundance in the UC biopsies are present in neutrophils and have been associated with the formation of neutrophil extracellular traps (NETs) (Table 3, asterisk indicates protein names).<sup>45</sup> NETs are a method of action by PMNs and are composed of extracellular fibrillar networks mainly of relaxed DNA and also contain proteins and other effector molecules, some of which have antimicrobial and antibody-like properties. NETs are released from PMNs in response to inflammatory stimuli, trapping the invading microorganisms, and facilitates interaction with other effector molecules that kill the microorganisms.<sup>45-47</sup> All 11 NET-associated proteins were found with increased abundance in the UC biopsies, and on average, the proteins were 42.2 times ( $P < 0.0005$ ) more abundant in the UC biopsies (Fig. 6).

## Confocal Laser Scanning Microscopy

To investigate if the increased abundance of PMN-associated proteins was a result of an increased abundance of PMNs, and if the PMNs were intact or found as NETs, we

investigated the TO-PRO-3 DNA-stained biopsy sections by confocal microscopy. The increased density of cell nuclei observed on the H&E-stained sections was again observed (Fig. 7), as was the segmented multilobulated nuclei, a characteristic of PMNs (Fig. 8A).<sup>42</sup> The PMNs were observed abundantly in biopsies from the UC group and occasionally in the control group. In addition to intact PMNs, we observed neutrophils that had excreted nuclear DNA into the extracellular environment forming NETs at 2 distinct locations in biopsies from UC\_4 (Fig. 8B).<sup>43</sup>

## DISCUSSION

The main result of this study is the identification of several novel proteins, which are present in increased abundance in the UC colonic tissue. Eleven of the proteins were associated with neutrophils and NETs, and the increased presence of both in the UC colonic tissue was verified with light microscopy and confocal microscopy.

Several studies have successfully analyzed different aspects of UC using genomic and transcriptomic techniques. However, sequencing techniques do not directly yield information about the abundance of the end product: the proteins, which are a combination of the newly synthesized and the degraded protein.<sup>11</sup> In our proteome analysis of colon mucosa biopsies from 10 patients with UC and 10 controls, we were able to quantify 5711 proteins in the colon mucosa biopsies, and the data quality was ensured by scatter plots and PCA. In previous studies, the amounts of calprotectin and lactotransferrin in feces have been found to correlate well with the degree of neutrophil infiltration and inflammation of the intestine.<sup>11,15</sup> We found that the abundance of these proteins in the colonic tissue correlated well with the colon inflammation grade scores, providing validation to the proteomics protein abundance data and the methodology. However, we found that the

**TABLE 3.** List of the 46 Proteins with a Statistically Significant Mean Abundance Change Between the UC Biopsies and Controls

Fold Change	Uniprot Acc.	Protein Name	Protein Function	Peptides (Unique), Seq. Cov.	MW	pI
219.2	P02788	Lactotransferrin*	Iron-binding protein with antimicrobial properties include bacteriostasis	51 (49), 72.7%	76,165	8.47
92.1	P14780	Matrix metalloproteinase-9*	Proteolysis of the extracellular matrix and leukocyte migration	30 (30), 51.8%	66,609	5.44
63.3	P05164	Myeloperoxidase*	Part of the defense system of PMN; responsible for microbicidal activity against a wide range of organisms	48 (41), 59.2%	66,107	9.22
31.4	P24158	Myeloblastin	PMN protease; degrades elastin, fibronectin, laminin, vitronectin, and collagen	7 (7), 36.3%	24,247	7.79
31.3	P08246	Neutrophil elastase*	Modifies functions of natural killer cells, monocytes, and granulocytes	11 (11), 54.7%	25,561	9.89
18.0	Q9NRD8	Dual oxidase 2	Lactoperoxidase-mediated antimicrobial defense at the surface of mucosa	42 (42), 33.6%	172,843	7.92
16.7	P11215	Integrin alpha-M	Adhesive interactions of monocytes, macrophages, and granulocytes	34 (33), 37.7%	125,471	6.75
16.3	P06702	Protein S100-A9*	One of the subunits in calprotectin; regulates inflammatory processes and immune response; Induce neutrophil chemotaxis, adhesion, increase bactericidal activity and degranulation	10 (10), 78.9%	13,110	5.71
13.7	P80188	Neutrophil gelatinase-associated lipocalin	Apoptosis, innate immunity, and renal development	12 (12), 63.6%	20,547	9.02
11.8	P80511	Protein S100-A12*	Regulates inflammatory processes and immune responses; recruitment of leukocytes, promotion of cytokine and chemokine production, and regulation of leukocyte adhesion and migration; antifungal and antimicrobial activity	5 (5), 35.9%	10,443	5.80
10.6	P22894	Neutrophil collagenase	Degradate fibrillar collagens	14 (14), 37.7%	41,937	5.49
9.9	P59666	Neutrophil defensin 3*	Fungicide, antiviral, and antimicrobial activity against bacteria	5 (5), 26.6%	3,492	8.33
9.4	P08637	Low-affinity immunoglobulin gamma Fc region receptor III-A	Binds monomeric, complexed, or aggregated IgG; mediates antibody-dependent responses (e.g., phagocytosis)	2 (2), 8.3%	27,324	8.24
9.2	P52790	Hexokinase-3	Metabolic processes; phosphorylation of hexoses	21 (18), 31.3%	99,025	5.23
8.7	O75594	Peptidoglycan recognition protein 1	Innate immunity; has bactericidal activity	5 (5), 41.3%	19,434	8.23
8.5	P36222	Chitinase-3-like protein 1	Regulates inflammatory cell apoptosis, dendritic cell accumulation, and macrophage differentiation; facilitates invasion of pathogenic enteric bacteria into colonic mucosa	14 (14), 44.9%	40,488	8.64
7.8	Q06141	Regenerating islet-derived protein 3-alpha	Antimicrobial activity against gram-positive bacteria	4 (4), 36.6%	16,566	7.83
7.3	Q1HG44	Dual oxidase maturation factor 2	Required for dual oxidase 2 maturation and transport to the plasma membrane	4 (4), 16.9%	34,786	8.51
6.6	Q05315	Galectin-10*	Regulates immune responses; recognition of cell surface glycans	11 (11), 67.6%	16,321	6.80
6.6	P35228	Nitric oxide synthase, inducible	Produces tumorcidal and bactericidal nitric oxide in macrophages	42 (41), 45.4%	131,117	8.20
6.2	P16050	Arachidonate 15-lipoxygenase	Regulates macrophage function and epithelial wound healing in the cornea; may favor clearance of apoptotic cells during inflammation	25 (25), 52.1%	74,673	6.14
5.9	P12724	Eosinophil cationic protein*	Antibacterial activity, including cytoplasmic membrane depolarization	10 (10), 46.9%	15,518	10.47
5.7	Q8IX19	Mast cell-expressed membrane protein 1	Integral component of membrane in mast cells (part of the immune system)	3 (3), 15.5%	21,228	9.03

**TABLE 3 (Continued)**

Fold Change	Uniprot Acc.	Protein Name	Protein Function	Peptides (Unique), Seq. Cov.	MW	pI
5.1	P10153	Nonsecretory ribonuclease	Pyrimidine-specific nuclease; selective chemotactic for dendritic cells	8 (8), 44.1%	15,463	9.20
5.0	P11678	Eosinophil peroxidase	Mediates tyrosine nitration of secondary granule proteins in mature eosinophils	51 (44), 56.8%	81,040	10.70
4.5	P41218	Myeloid cell nuclear differentiation antigen*	Plays a role in the granulocyte/monocyte response to interferon	17 (17), 39.1%	45,836	9.76
4.4	P06310	Ig kappa chain V-II region RPMI 6410	Immunoregulatory interactions between a lymphoid and a nonlymphoid cell	4 (3), 37.6%	12,585	9.07
4.3	Q8TCU6	Phosphatidylinositol-3,4,5-trisphosphate-dependent Rac exchanger	Neutrophil chemotaxis; may function downstream of heterotrimeric G proteins in neutrophils	8 (8), 6.4%	186,203	6.03
4.0	P01040	Cystatin-A	Intracellular thiol proteinase inhibitor; desmosome-mediated cell-cell adhesion in the lower epidermis levels	2 (2), 30.6%	10,875	5.39
4.0	Q96Q80	Derlin-3	Functional component of endoplasmic reticulum-associated degradation for misfolded luminal glycoproteins	4 (3), 26.8%	26,678	8.64
3.9	Q7Z7N9	Transmembrane protein 179B	Integral component of membrane	2 (2), 8.2%	23,550	8.10
3.8	Q70J99	Protein unc-13 homolog D	Regulates secretory lysosome exocytosis in mast cells and cytotoxic granule exocytosis in lymphocytes; required for granule maturation and docking	16 (16), 24.7%	123,281	6.19
3.5	P08311	Cathepsin G*	Serine protease; cleaves complement C3; has antibacterial activity against the gram-negative bacterium <i>Pseudomonas aeruginosa</i>	16 (16), 54.1%	26,757	11.37
0.4	P29966	Myristoylated alanine-rich C-kinase substrate	Filamentous actin cross-linking protein; binds calmodulin, actin, and synapsin	11 (11), 49.1%	31,423	4.46
0.3	P00326	Alcohol dehydrogenase 1C	Oxidation of alcohol	27 (10), 64.8%	39,868	8.63
0.3	P20039	HLA class II histocompatibility antigen, DRB1-11 beta chain	Binds peptides derived from antigens that access the endocytic route of antigen-presenting cells and presents them on the cell surface for recognition	9 (2), 40.6%	27,230	6.49
0.3	P10082	Peptide YY	Gut peptide; inhibits exocrine pancreatic secretion, and jejunal and colonic motility; has vasoconstrictory action	3 (3), 29.9%	4,410	8.34
0.3	Q12805	EGF-containing fibulin-like extracellular matrix protein 1	May play a role in cell adhesion and migration; binds the EGF receptor, inducing phosphorylation and activation	15 (15), 43.0%	52,765	4.85
0.3	Q9HBI6	Phylloquinone omega-hydroxylase CYP4F11	Oxidizes a variety of compounds, including fatty acids and xenobiotics; may play a role in blood coagulation	11 (3), 26.7%	60,146	6.26
0.3	P15502	Elastin	Major structural protein of tissues; regulates proliferation and organization of vascular smooth muscles	6 (6), 17.7%	65,721	10.32
0.3	P10915	Hyaluronan and proteoglycan link protein 1	Stabilizes the aggregates of proteoglycan monomers with hyaluronic acid in the extracellular cartilage matrix	14 (13), 48.6%	38,840	6.85
0.2	Q86Y39	NADH dehydrogenase (ubiquinone) 1 alpha subcomplex subunit 11	Subunit of the mitochondrial membrane respiratory chain NADH dehydrogenase, thought not to be involved in catalysis	7 (7), 58.2%	14,721	8.95

**TABLE 3 (Continued)**

Fold Change	Uniprot Acc.	Protein Name	Protein Function	Peptides (Unique), Seq. Cov.	MW	pI
0.2	P35558	Phosphoenolpyruvate carboxykinase, cytosolic (GTP)	Catalyzes conversion of oxaloacetate to phosphoenolpyruvate, the rate-limiting step in the metabolic pathway that produces glucose from lactate and other precursors from the citric acid cycle	38 (34), 71.4%	69,195	5.8
0.2	Q6PIJ6	F-box only protein 38	Thought to recognize and bind to some phosphorylated proteins and promotes their ubiquitination and degradation	6 (6), 7.0%	133,944	5.92
0.2	Q07654	Trefoil factor 3	Involved in the maintenance and repair of the intestinal mucosa; promotes the mobility of epithelial cells in healing	3 (3), 38.8%	6580	5.13
0.2	Q14508	WAP four-disulfide core domain protein 2	Broad range protease inhibitor	4 (4), 45.2%	10,036	4.50

Fold change  $>1$  indicates increased mean abundance in the UC biopsies compared with controls.

\*Protein has been associated with NETs.<sup>46</sup> The number of identified peptides, the resulting sequence coverage (seq. cov), and the number of unique peptides used for the quantitation are listed for each protein. Protein functions have been downloaded from Uniprot Knowledgebase, and molecular weight (MW) in daltons and isoelectric point (pI) have been downloaded from ExPASy. EGF, epidermal growth factor; GTP, guanosine triphosphate.

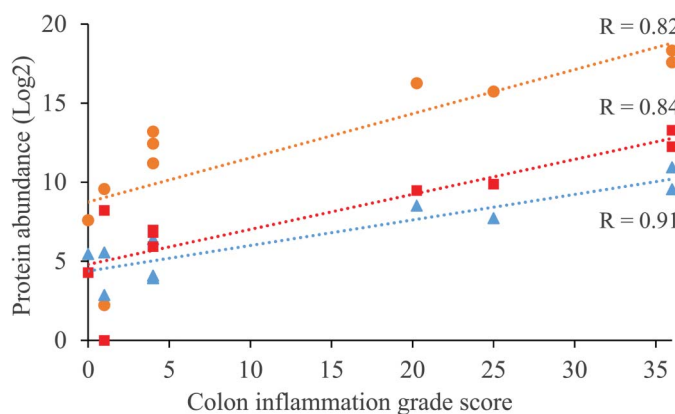


**FIGURE 5.** Correlation analysis of inflammatory proteins. Colon inflammation grade scores and the protein abundance in the colon tissue of the inflammatory proteins lactotransferrin (●), S100-A8 (■), and S100-A9 (▲) (S100-A8 and S100-A9 protein constitute calprotectin).

amount of fecal calprotectin did not correlate with the colon inflammation grade scores or the measured amount of calprotectin in the tissue (data not shown), which have been reported by others.<sup>48</sup> A likely explanation is that the measure of fecal calprotectin and the biopsy extraction was not conducted in parallel in the present study, and only for 3 of the 10 patients with UC were the fecal calprotectin measures obtained on the day. Additionally, fecal calprotectin is a marker for inflammation in the entire intestinal system, in contrast to the colon inflammation grade score and the proteomics analysis where the transverse colon or the

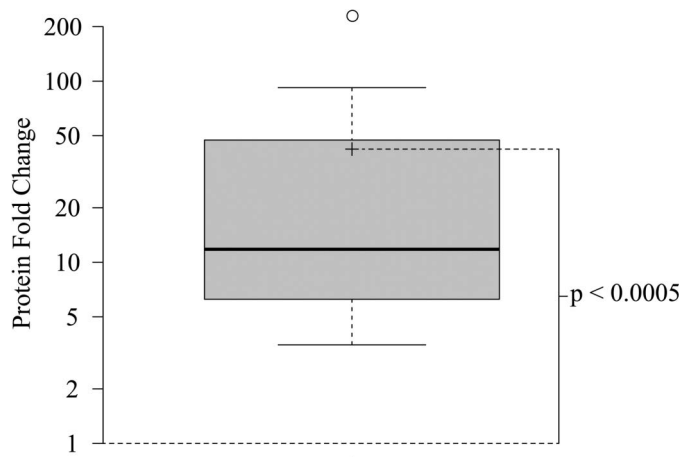


**FIGURE 6.** Fold change of statistically significantly changing NET-associated proteins between biopsies from the patients with UC and controls. The 11 proteins are on average 42.2 times ( $P < 0.0005$ ) more abundant in the biopsies from the UC group compared with the biopsies from the control group. Center line shows the median, box limits indicate the 25th and 75th percentiles, whiskers extend 1.5 times the interquartile range from the 25th and 75th percentiles, crosses represent sample means, and the circle represents the fold change of lactotransferrin that lies outside the whiskers.

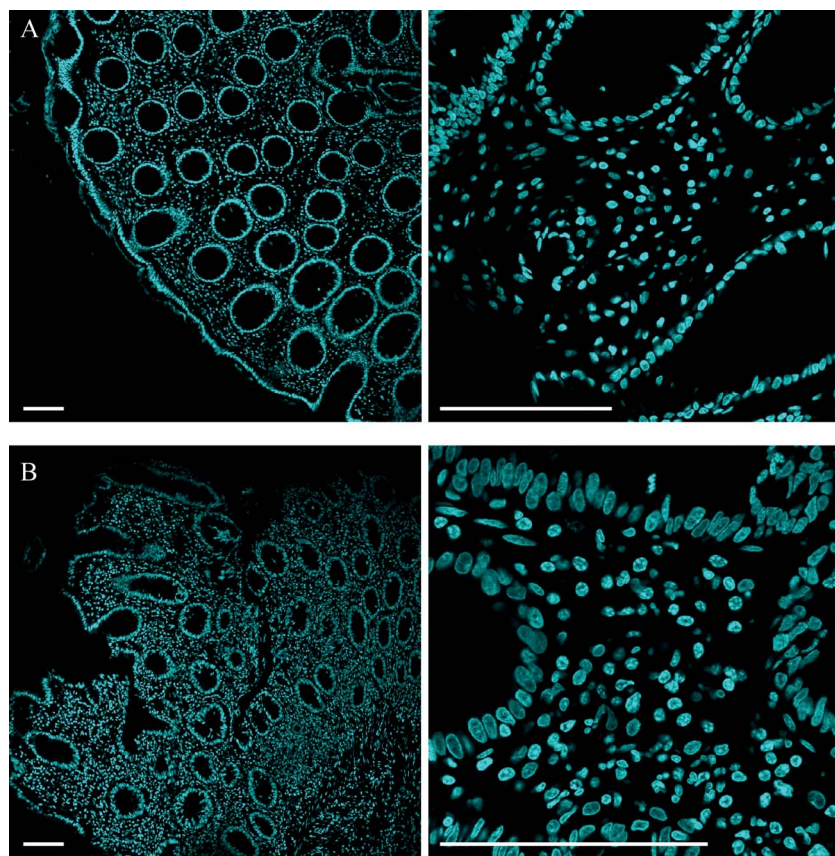


**FIGURE 7.** Confocal microscopic images of TO-PRO-3-stained biopsy slices (scale bars 100  $\mu$ m): (A) Ctrl\_5 and (B) UC\_3. An increased number of stained cell nuclei surrounding the intestinal crypts are in general apparent in the UC biopsies compared with the control biopsies.

ascending colon was not considered. This is likely why, for example, patient UC\_4 treated with suppository Pentasa had a colon inflammation grade score of 1, indicating for the most part healthy looking biopsies. However, >3600  $\mu$ g of fecal calprotectin per gram stools was measured indicating inflammation in the transverse colon or the ascending colon, too far from the rectum for the treatment with suppository Pentasa to have an effect. Finally, it has been reported that fecal calprotectin can be increased 3 months before a disease flare.<sup>49</sup> As the patients in this study were not followed up after the biopsy was taken, it cannot be excluded that these patients later could have developed disease flares, which caused the elevated fecal calprotectin.

Of the 5711 quantifiable proteins, 46 proteins were measured to have a statistically significant change in abundance between the biopsies from the patients with UC and the controls. Of these, 33 proteins were more abundant in the UC biopsies. Several of the proteins with a statistically significant abundance increase were involved in inflammation. On comparison with the only other gel-free LC-MS study conducted, we found several proteins that were determined to be more abundant in the UC colon tissue in both studies, namely, Protein S100-A9 (calprotectin), neutrophil elastase, myeloperoxidase, neutrophil defensin, and cathepsin G.<sup>20</sup> These consistent findings validate the study. However, the study by Han et al<sup>20</sup> additionally reported that a number of histones and fibrinogen

proteins were more abundant. These proteins were identified and quantified in the present study; however, we could not confirm the increased abundance. However, our study found several proteins associated with the innate immune system to be increased in abundance in the UC colonic tissue. The differences between findings in the 2 studies are mainly ascribed to differences in the obtained patient material and study design. The advantages of a state-of-the-art instrument and bioinformatics platform are demonstrated in the increase from up to 339 proteins in the study by Han et al<sup>20</sup> to the 5711 quantifiable proteins in the present study, thus providing information on the regulation of a great number of proteins and thus cellular functions. A potential drawback of the high number of quantifiable proteins is that a large number of *t* tests need to be performed during the statistical analysis. To avoid a high number of false positives among the proteins found to be statistically significant, multiple hypothesis testing must be applied, which increases the requirements for the *P*-values.<sup>21</sup> As a consequence, when many proteins are quantified and analyzed, the statistical analysis results in the need for a higher number of included subjects in the study. As an example, an overabundance of the enzyme indoleamine-2,3-dioxygenase has been found in intestinal mucosal tissue from patients with IBD compared with normal mucosa, hypothesizing an involvement of the Kynurenine pathway of tryptophan metabolism in the IBDs.<sup>50,51</sup>

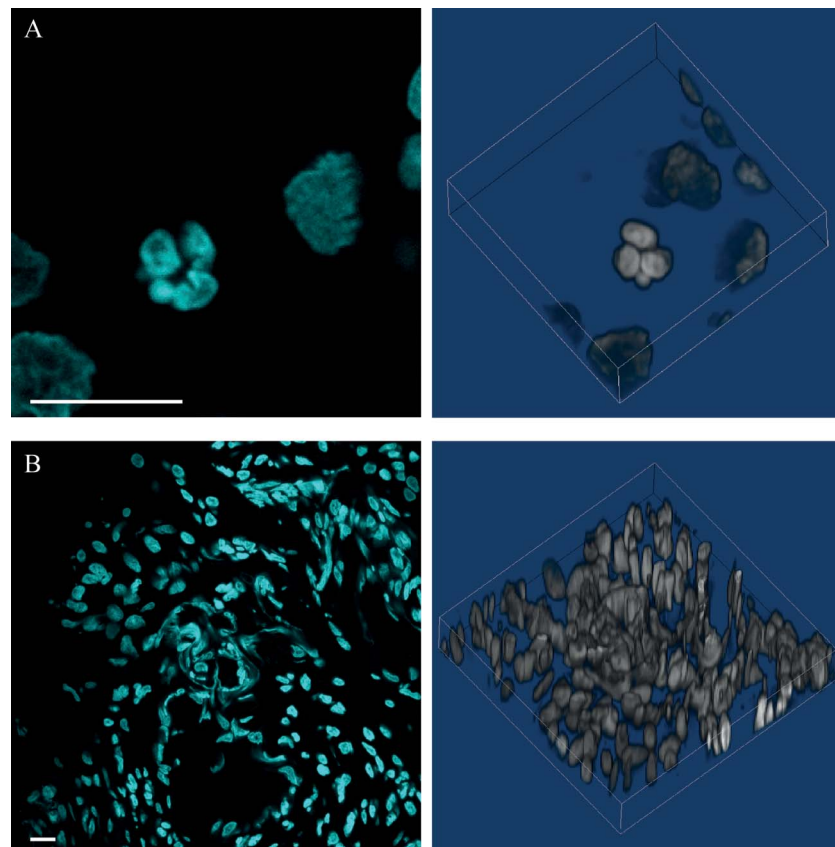


**FIGURE 8.** Confocal microscopy images of TO-PRO-3-stained biopsy slices from the UC group (scale bars 100  $\mu$ m): (A) UC\_6 with an intact neutrophil, with segmented multilobulated-shaped nucleus; (B) UC\_4 with NET formation by excretion of the neutrophil DNA.

Indoleamine-2,3-dioxygenase is an intracellular enzyme that catalyzes the production of Kynurenine from the amino acid tryptophan. The enzyme is regulated by gamma-interferon of the immune system.<sup>52</sup> The protein in our study was detected with a 1.8 mean fold abundance increase in the UC biopsies compared with controls but not statistically significant. This indicates that a larger study cohort could have identified a higher number of statistically significantly changed proteins.

Gel-free quantitative LC-MS studies hold a number of advantages over 1- and 2-dimensional gel-based approaches, including increased sensitivity, increased dynamic range, and identification and quantification of proteins in the thousands instead of hundreds. However, the gel-free approaches such as the present study are limited in the ability to detect protein fragment products.<sup>11,19</sup> The increased sensitivity of the gel-free approaches becomes apparent when considering that the gel-free LC-MS method used in this study analyzed 5  $\mu$ g of the final material compared with the hundreds of microgram material used for the 2-dimensional gel analysis, which allowed us to conduct repeated analysis of each biopsy.<sup>17,53</sup> Two-dimensional gel studies are usually limited to proteins within a molecular mass range of 15 to 200 kDa and isoelectric point of the proteins in the range of 3 to 10. These limitations do not apply for gel-free approaches, and applying these criteria to the 46 proteins detected with a statistically significant change in this study 30.4% (14 proteins) would not be

detectable with 2-dimensional gel studies (Table 3).<sup>11,19</sup> This includes protein S100-A12, which was found to be 11.8-fold increased in the UC colonic tissue and also has been found elevated in the serum of children with IBD.<sup>54</sup> Interestingly, the present study is the first MS-driven proteomics study to measure an increased abundance of lactotransferrin in the UC colonic tissue. The increased abundance of fecal lactotransferrin is used as a marker for inflammation, and the protein should have been detectable using 2-dimensional gel-based analysis.<sup>11,55</sup> However, it is possible that the relative abundance of this protein remains too low for gel-based studies. Nonetheless, the protein abundance in the colonic tissue correlates well with the abundance of calprotectin in the tissue, and the colon inflammation grade scores in this study, as expected.<sup>11,55</sup> Another protein involved in inflammation and found with increased abundance in the UC biopsies is myeloblastin. Myeloblastin is a protease found in neutrophils and was found to be 31.4-fold more abundant in the UC colonic biopsies compared with controls. The protease has specificity toward, among others, the protein elastin, which accordingly has a decreased abundance in the UC biopsies, with a 1/3.3-fold change. Another interesting protein found with 8.7-fold increase in abundance in the UC colonic biopsies is peptidoglycan recognition protein 1. The protein is part of the innate immune

systems recognition of microorganisms and mediates its effect by binding bacterial peptidoglycans, which triggers a signaling cascade.<sup>56,57</sup> This is the first study to find an increased abundance of peptidoglycan recognition protein 1 in UC colonic tissue. Hexokinase-3 is an intracellular enzyme that phosphorylates glucose into glucose-6-phosphate and, together with hexokinase 1, 2, and 4, is a central rate-limiting step in glucose metabolism.<sup>58,59</sup> Not much is known about the regulation of hexokinase 3; however, the 9.2-fold increased abundance of this enzyme in the UC biopsies indicates that glucose metabolism might be increased in the inflamed tissue compared with controls.

The increased abundance of inflammation-associated proteins points to an activated innate immune system in the UC colon, even in colonic tissue without visible inflammation. It should be noted that we do not know the impact of the medication on the protein regulations. However, as most of the statistically significant changed proteins are involved in inflammatory processes, these protein changes are likely caused by the disease development. Additionally, the number of former smokers was increased in the UC group compared with controls. The impact of cigarette smoking on the etiology of UC has been vastly debated over the years.<sup>60–65</sup> Current knowledge supports that the risk for developing UC is highest 2 to 5 years after smoking cessation and remains elevated for more than 20 years, and patients with UC are more prone to disease flairs if they quit smoking.<sup>60</sup> However, the subject is still debated and the dose-response effect remains to be properly determined. Based on the present study, we cannot assess the impact of former smoking on the protein data.

To evaluate the morphology of the tissue, the biopsies were sectioned and H&E stained, and the histological evaluation was done by light microscopy. The intestinal crypts were preserved in all biopsies, in agreement with the biopsies being taken from morphologically normal tissue. However, an increased abundance of cell nuclei in the colon mucosal tissue was observed between the intestinal crypts, with segmented cell nuclei, a characteristic of PMNs. Based on the proteomics data and light microscopy, we here verify the increased density of PMNs in the UC colonic tissue. This has been reported by other groups as well, but this is the first study to support the light microscopy identification of the PMNs with MS techniques.<sup>66,67</sup> PMNs are essential for the innate immunity and are the most abundant leukocyte in plasma. In response to inflammatory stimuli, they migrate from plasma to the affected tissue where they take part in the first line of innate immune response. The effect is mediated through the release of enzymes from the granules and the production of compounds with antimicrobial potential and inflammation regulatory effects.<sup>15</sup> One of the compounds is NET. PMNs can disintegrate their cell membrane and release NETs to capture and kill invasive microorganisms.<sup>47,68</sup> The NETs are composed of relaxed DNA to which histones and other effector molecules are bound.<sup>45</sup> Eleven of the 46 proteins with statistically significantly altered abundance in the UC biopsies are associated with NET formation, and all were measured with increased abundance. As no proteins unique to NETs are known, we investigated if the PMNs were intact or

found as NETs. We stained the biopsy sections with a DNA stain and investigated the sections by confocal microscopy, which allowed us to achieve a higher resolution than with light microscopy. Again, the segmented cell nucleus of the PMNs was apparent, and additionally, in biopsies from UC\_4, we observed NETs at 2 distinct locations. The proteomics data and microscopy data demonstrate the increased abundance of PMNs in UC colon tissue and NETs in biopsies from UC\_4. This study is the first to directly observe NETs in UC colon tissue. Interestingly, the abundances of several NET-associated histone proteins (H1e, H2A, H2B, H3, and H4) were not found with increased abundance in the UC biopsies.<sup>45</sup> Additionally, histones H2A and H3 were found to be more abundant in the UC colonic tissue by Han et al<sup>20</sup> indicating that NETs could have been present in the colonic tissue obtained in this study as well. However, as histone proteins are an essential part of nearly all cells, a relative increase in the abundance of these proteins between the UC biopsies and controls as a result of the presence of NETs might be too small to be detected.

NETs are part of the innate immune system's response to invading pathogens.<sup>47,68</sup> Additionally, several of proteins found to be more abundant in the UC colon tissue are directly involved in the mucosal innate immune system response. However, the cause for the immune response remains unknown, and no indications of bacteria or epithelial cell disruption were detected by the histology analysis, which should have been visible using confocal microscopy. It cannot be ruled out that the immune reactions could be caused by bacterial components capable of crossing the intestinal barrier of epithelial cells, which is known to be compromised in IBD where an increased epithelial permeability has been described.<sup>10,69,70</sup> However, it has been demonstrated that aberrant formation of NETs might be involved in the pathogenesis of autoimmunity and additionally might be formed during a number of activities, including exercise.<sup>71–73</sup> Therefore, based on the obtained data in this study, we can conclude that a chronic inflammation is present in the tissue, even though the surface appears normal. However, we cannot point to the origin of the inflammation or the target of the immune response.

Our findings demonstrate that even though remission has been achieved on the surface of the UC colonic tissue, a chronic condition is still present within the tissue. Poulsen et al<sup>18</sup> performed a 2-dimensional proteomics study of 20 patients with UC where inflamed and noninflamed tissue from the same patient with UC were compared, in contrast to the present study where noninflamed tissue from several patients with UC was compared with controls.<sup>18</sup> Interestingly, the study by Poulsen et al<sup>18</sup> found that in contrast to the macroscopically different tissue, the proteome of visually inflamed and noninflamed tissue was only slightly different. Of the 43 protein spots identified with a different abundance, the protein displaying the largest fold change was glycerol-3-phosphate dehydrogenase, which was increased by 3.3-fold in the inflamed UC tissue compared with noninflamed tissue, which is a minor change compared with the up to 219-fold changes measured in the present study. Combined with the analysis of differences in colonic proteome between patients with UC

and controls, we can conclude that the difference in proteome between visually inflamed and noninflamed UC colonic tissue is vastly smaller than the interpersonal difference between patients with UC and controls. This indicates that changes are present in the UC colonic tissue regardless of visible surface inflammation, even in well-medicated patients with UC. A 2012 Danish population-based cohort study of 300 patients with UC in the period of 2003 to 2011, found that even though intensified immunomodulation therapy is being used in Denmark, the first time recurrence rate, hospitalization rate, and surgical rates for patients with UC have not decreased.<sup>74</sup> This observation supports the hypothesis that the administered treatment mostly is symptomatic. However, it is worth mentioning that a study by Reich et al,<sup>75</sup> in which 481 patients with UC undergoing colectomy in the period 1998 to 2011 were included, showed that following the approval of anti-tumor necrosis factor treatment for UC in 2005, the colectomy rate has dropped.<sup>75</sup> None of the patients included in this study had active disease or was under treatment with anti-tumor necrosis factor substances. Nonetheless, based on our study, we can conclude that chronic inflammation remains in the UC colonic tissue.

In conclusion, we have found an increased abundance of PMNs in the UC colonic tissue, using high-throughput proteomics, light microscopy, and confocal microscopy. Additionally, we have for the first time observed NETs, detected by proteomics and verified by light microscopy at 2 distinct locations in a biopsy from a patient with UC. Our findings demonstrate an activated innate immune system in well-medicated patients with UC without disease activity and the presence of chronic inflammation in the morphologically normal tissue. Additionally, through a comparison with other studies, we can conclude that the proteome of inflamed and noninflamed tissue from the same patient is much more similar compared with the proteome of different individuals, indicating that a chronic condition is present even in UC colonic tissue that appears normal during endoscopy. However, no indications of bacterial infiltrations in the tissue were found in the study. To increase our understanding of the UC and IBD etiology, future studies should aim at investigating the etiology of the immune reaction in the UC colonic tissue.

## ACKNOWLEDGMENTS

Knud and Edith Eriksens Memorial Foundation and Ferring are acknowledged for grants, enabling the collection of the biological sample material (V.A.). The Obelske Family Foundation and the Svend Andersen Foundation are acknowledged for grants supporting the analytical platform (A.S.). Knud Hojgaards Foundation Denmark, the Lundbeck Foundation Denmark, the Oticon Foundation Denmark, and the Otto Monsteds Foundation Denmark are acknowledged for grants supporting the collaboration (T.B.B.). Additionally, the authors would like to thank Kasper B. Lauridsen for help establishing the patient cohort, Lau Sennels for help with the data analysis, Professor Mogens Vyberg for help interpreting the histology descriptions, and the PRIDE team for making the proteomics data publically available.

## REFERENCES

- Molodecky NA, Soon IS, Rabi DM, et al. Increasing incidence and prevalence of the inflammatory bowel diseases with time, based on systematic review. *Gastroenterology*. 2012;142:46–54.e42.
- Odes S, Vardi H, Friger M, et al. Cost analysis and cost determinants in a European inflammatory bowel disease inception cohort with 10 years of follow-up evaluation. *Gastroenterology*. 2006;131:719–728.
- Jess T, Frisch M, Simonsen J. Trends in overall and cause-specific mortality among patients with inflammatory bowel disease from 1982 to 2010. *Clin Gastroenterol Hepatol*. 2013;11:43–48.
- Jussila A, Virta LJ, Pukkala E, et al. Mortality and causes of death in patients with inflammatory bowel disease: a nationwide register study in Finland. *J Crohns Colitis*. 2014;8:1088–1096.
- Khor B, Gardet A, Xavier RJ. Genetics and pathogenesis of inflammatory bowel disease. *Nature*. 2011;474:307–317.
- Iskandar HN, Ciorka MA. Biomarkers in inflammatory bowel disease: current practices and recent advances. *Transl Res*. 2012;159:313–325.
- Ehrentraut SF, Colgan SP. Implications of protein post-translational modifications in IBD. *Inflamm Bowel Dis*. 2012;18:1378–1388.
- Thompson AI, Lees CW. Genetics of ulcerative colitis. *Inflamm Bowel Dis*. 2011;17:831–848.
- Jostins L, Ripke S, Weersma RK, et al. Host-microbe interactions have shaped the genetic architecture of inflammatory bowel disease. *Nature*. 2012;491:119–124.
- Xavier RJ, Podolsky DK. Unravelling the pathogenesis of inflammatory bowel disease. *Nature*. 2007;448:427–434.
- Bennike T, Birkeland S, Stensballe A, et al. Biomarkers in inflammatory bowel diseases: current status and proteomics identification strategies. *World J Gastroenterol*. 2014;20:3231–3244.
- Tontini GE, Vecchi M, Pastorelli L, et al. Differential diagnosis in inflammatory bowel disease colitis: state of the art and future perspectives. *World J Gastroenterol*. 2015;21:21–46.
- Kane SV, Sandborn WJ, Rufo PA, et al. Fecal lactoferrin is a sensitive and specific marker in identifying intestinal inflammation. *Am J Gastroenterol*. 2003;98:1309–1314.
- Mendoza JL, Abreu MT. Biological markers in inflammatory bowel disease: practical consideration for clinicians. *Gastroenterol Clin Biol*. 2009; 33(suppl 3):S158–S173.
- Johns B, Fagerhol MK, Lyberg T, et al. Functional and clinical aspects of the myelomonocyte protein calprotectin. *Mol Pathol*. 1997;50:113–123.
- Steinbakk M, Naess-Andresen C-F, Fagerhol MK, et al. Antimicrobial actions of calcium binding leucocyte L1 protein, calprotectin. *Lancet*. 1990;336:763–765.
- Hsieh SY, Shih TC, Yeh CY, et al. Comparative proteomic studies on the pathogenesis of human ulcerative colitis. *Proteomics*. 2006;6:5322–5331.
- Poulsen NA, Andersen V, Møller JC, et al. Comparative analysis of inflamed and non-inflamed colon biopsies reveals strong proteomic inflammation profile in patients with ulcerative colitis. *BMC Gastroenterol*. 2012;12:76.
- Camerini S, Mauri P. The role of protein and peptide separation before mass spectrometry analysis in clinical proteomics. *J Chromatogr A*. 2015; 1381:1–12.
- Han NY, Choi W, Park JM, et al. Label-free quantification for discovering novel biomarkers in the diagnosis and assessment of disease activity in inflammatory bowel disease. *J Dig Dis*. 2013;14:166–174.
- Krzywinski M, Altman N. Points of significance: comparing samples—part II. *Nat Methods*. 2014;11:355–356.
- Dignass A, Eliakim R, Magro F, et al. Second European evidence-based consensus on the diagnosis and management of ulcerative colitis part 1: definitions and diagnosis. *J Crohns Colitis*. 2012;6:965–990.
- Fernández-Baños F, Casalots J, Salas A, et al. Paucicellular lymphocytic colitis: is it a minor form of lymphocytic colitis? A clinical pathological and immunological study. *Am J Gastroenterol*. 2009;104:1189–1198.
- Schneider CA, Rasband WS, Eliceiri KW. NIH Image to ImageJ: 25 years of image analysis. *Nat Methods*. 2012;9:671–675.
- Hanauer SB, Robinson M, Pruitt R, et al. Budesonide enema for the treatment of active, distal ulcerative colitis and proctitis: a dose-ranging study. *Gastroenterology*. 1998;115:525–532.
- Leon IR, Schwammlle V, Jensen ON, et al. Quantitative assessment of in-solution digestion efficiency identifies optimal protocols for unbiased protein analysis. *Mol Cell Proteomics*. 2013;12:2992–3005.

27. Wisniewski JR, Zougman A, Nagaraj N, et al. Universal sample preparation method for proteome analysis. *Nat Methods*. 2009;6:359–362.
28. Manza LL, Stamer SL, Ham AJL, et al. Sample preparation and digestion for proteomic analyses using spin filters. *Proteomics*. 2005;5:1742–1745.
29. Masuda T, Tomita M, Ishihama Y. Phase transfer surfactant-aided trypsin digestion for membrane proteome analysis. *J Proteome Res*. 2008;7:731–740.
30. Urbaniak GC, Plous S. *Research Randomizer (Version 4.0)* [computer software]. 2013. Available at: <http://www.randomizer.org/>. Accessed October 10, 2013.
31. Cox J, Mann M. MaxQuant enables high peptide identification rates, individualized p.p.b.-range mass accuracies and proteome-wide protein quantification. *Nat Biotech*. 2008;26:1367–1372.
32. Cox J, Neuhauser N, Michalski A, et al. Andromeda: a peptide search engine integrated into the MaxQuant environment. *J Proteome Res*. 2011; 10:1794–1805.
33. Bennike T, Ayturk U, Haslauer CM, et al. A normative study of the synovial fluid proteome from healthy porcine knee joints. *J Proteome Res*. 2014;13:4377–4387.
34. Bennike T, Lauridsen KB, Olesen MK, et al. Optimizing the identification of citrullinated peptides by mass spectrometry: utilizing the inability of trypsin to cleave after citrullinated amino acids. *J Proteomics Bioinform*. 2013;06:288–295.
35. Deeb SJ, D’Souza RCJ, Cox J, et al. Super-silac allows classification of diffuse large B-cell lymphoma subtypes by their protein expression profiles. *Mol Cell Proteomics*. 2012;11:77–89.
36. Bhatia VN, Perlman DH, Costello CE, et al. Software tool for researching annotations of proteins: open-source protein annotation software with data visualization. *Anal Chem*. 2009;81:9819–9823.
37. Tusher VG, Tibshirani R, Chu G. Significance analysis of microarrays applied to the ionizing radiation response. *Proc Natl Acad Sci U S A*. 2001;98:5116–5121.
38. Hubner NC, Bird AW, Cox J, et al. Quantitative proteomics combined with BAC TransgeneOmics reveals in vivo protein interactions. *J Cell Biol*. 2010;189:739–754.
39. Murgia M, Nagaraj N, Deshmukh AS, et al. Single muscle fiber proteomics reveals unexpected mitochondrial specialization. *EMBO Rep*. 2015; 16:387–395.
40. Vizcaíno JA, Deutsch EW, Wang R, et al. ProteomeXchange provides globally coordinated proteomics data submission and dissemination. *Nat Biotechnol*. 2014;32:223–226.
41. Vizcaíno JA, Côté RG, Csordas A, et al. The PRoteomics IDEntifications (PRIDE) database and associated tools: status in 2013. *Nucleic Acids Res*. 2013;41:D1063–D1069.
42. Fournier BM, Parkos CA. The role of neutrophils during intestinal inflammation. *Mucosal Immunol*. 2012;5:354–366.
43. Brinkmann V, Zychlinsky A. Neutrophil extracellular traps: is immunity the second function of chromatin? *J Cell Biol*. 2012;198:773–783.
44. Rao PK, Li Q. Principal component analysis of proteome dynamics in iron-starved mycobacterium tuberculosis. *J Proteomics Bioinform*. 2009; 2:19–31.
45. O’Donoghue AJ, Jin Y, Knudsen GM, et al. Global substrate profiling of proteases in human neutrophil extracellular traps reveals consensus motif predominantly contributed by Elastase Glogauer M, ed. *PLoS One*. 2013; 8:e75141.
46. Mantovani A, Cassatella MA, Costantini C, et al. Neutrophils in the activation and regulation of innate and adaptive immunity. *Nat Rev Immunol*. 2011;11:519–531.
47. Brinkmann V, Reichard U, Goosmann C, et al. Neutrophil extracellular traps kill bacteria. *Science*. 2004;303:1532–1535.
48. Schoepfer AM, Beglinger C, Straumann A, et al. Fecal calprotectin more accurately reflects endoscopic activity ulcerative colitis than Lichtiger Index, C-reactive protein platelets, hemoglobin, and blood leukocytes. *Inflamm Bowel Dis*. 2013;19:332–341.
49. Vos MD, Louis EJ, Jahnson J, et al. Consecutive fecal calprotectin measurements predict relapse patients ulcerative colitis receiving infliximab maintenance therapy. *Inflamm Bowel Dis*. 2013;19:2111–2117.
50. Barceló-Batllo S, André M, Servis C, et al. Proteomic analysis of cytokine induced proteins in human intestinal epithelial cells: implications for inflammatory bowel diseases. *Proteomics*. 2002;2:551–560.
51. Munn DH, Mellor AL. Indoleamine 2,3 dioxygenase and metabolic control of immune responses. *Trends Immunol*. 2013;34:137–143.
52. Schmidt SV, Schultze JL. New insights into IDO biology in bacterial and viral infections. *Front Immunol*. 2014;5:384.
53. Shkoda A, Werner T, Daniel H, et al. Differential protein expression profile in the intestinal epithelium from patients with inflammatory bowel disease. *J Proteome Res*. 2007;6:1114–1125.
54. Leach ST, Yang Z, Messina I, et al. Serum and mucosal S100 proteins, calprotectin (S100A8/S100A9) and S100A12, are elevated at diagnosis in children with inflammatory bowel disease. *Scand J Gastroenterol*. 2007; 42:1321–1331.
55. Lehmann FS, Burri E, Beglinger C. The role and utility of faecal markers in inflammatory bowel disease. *Therap Adv Gastroenterol*. 2015;8:23–36.
56. Lu X, Wang M, Qi J, et al. Peptidoglycan recognition proteins are a new class of human bactericidal proteins. *J Biol Chem*. 2006;281:5895–5907.
57. Liu C, Xu Z, Gupta D, et al. Peptidoglycan recognition proteins a novel family of four human innate immunity pattern recognition molecules. *J Biol Chem*. 2001;276:34686–34694.
58. Furuta H, Nishi S, Le Beau MM, et al. Sequence of human hexokinase III cDNA and assignment of the human hexokinase III gene (HK3) to chromosome band 5q35.2 by fluorescence in situ hybridization. *Genomics*. 1996;36:206–209.
59. Lowes W, Walker M, Alberti KG, et al. Hexokinase isoenzymes in normal and cirrhotic human liver: suppression of glucokinase in cirrhosis. *Biochim Biophys Acta*. 1998;1379:134–142.
60. Rosenfeld G, Bressler B. The truth about cigarette smoking and the risk of inflammatory bowel disease. *Am J Gastroenterol*. 2012;107:1407–1408.
61. Higuchi LM, Khalili H, Chan AT, et al. A Prospective study of cigarette smoking and the risk of inflammatory bowel disease in women. *Am J Gastroenterol*. 2012;107:1399–1406.
62. Abraham C, Cho JH. Inflammatory bowel disease. *N Engl J Med*. 2009; 361:2066–2078.
63. Mahid SS, Minor KS, Soto RE, et al. Smoking and inflammatory bowel disease: a meta-analysis. *Mayo Clin Proc*. 2006;81:1462–1471.
64. García Rodríguez LA, González-Pérez A, Johansson S, et al. Risk factors for inflammatory bowel disease in the general population. *Aliment Pharmacol Ther*. 2005;22:309–315.
65. Lindberg E, Tysk C, Andersson K, et al. Smoking and inflammatory bowel disease. A case control study. *Gut*. 1988;29:352–357.
66. Khor TS, Fujita H, Nagata K, et al. Biopsy interpretation of colonic biopsies when inflammatory bowel disease is excluded. *J Gastroenterol*. 2012;47:226–248.
67. Geboes K. Histopathology of Crohn’s disease and ulcerative colitis. *Inflamm Bowel Dis*. 2003;255–276.
68. Branzk N, Lubojemska A, Hardison SE, et al. Neutrophils sense microbe size and selectively release neutrophil extracellular traps in response to large pathogens. *Nat Immunol*. 2014;15:1017–1025.
69. Fava F, Danese S. Intestinal microbiota in inflammatory bowel disease: friend or foe? *World J Gastroenterol*. 2011;17:557–566.
70. Tlaskalová-Hogenová H, Štěpánková R, Hudcová T, et al. Commensal bacteria (normal microflora), mucosal immunity and chronic inflammatory and autoimmune diseases. *Immunol Lett*. 2004;93:97–108.
71. Beiter T, Fragasso A, Hartl D, et al. Neutrophil extracellular traps: a walk on the wild side of exercise immunology. *Sports Med*. 2015;45:625–640.
72. Beiter T, Fragasso A, Hudemann J, et al. Neutrophils release extracellular DNA traps in response to exercise. *J Appl Physiol (1985)*. 2014; 117:325–333.
73. Stephan A, Fabri M. The NET, the trap, and the pathogen: neutrophil extracellular traps in cutaneous immunity. *Exp Dermatol*. 2014;24: 161–166.
74. Vester-Andersen MK, Vind I, Prosberg MV, et al. Hospitalisation, surgical and medical recurrence rates in inflammatory bowel disease 2003–2011—a Danish population-based cohort study. *J Crohns Colitis*. 2014;8: 1675–1683.
75. Reich KM, Chang H-J, Rezaie A, et al. The incidence rate of colectomy for medically refractory ulcerative colitis has declined in parallel with increasing anti-TNF use: a time-trend study. *Aliment Pharmacol Ther*. 2014;40:629–638.